A Simple Approximate Result for the Maximum Growth Rate of Baroclinic Instabilities

R. S. LINDZEN AND BRIAN FARRELL

Center for Earth and Planetary Physics, Harvard University, Cambridge, MA 02138

8 November 1979 and 4 February 1980

ABSTRACT

The Charney problem for baroclinic instability involves the quasi-geostrophic instability of a zonal flow on a β plane where the zonal flow is characterized by a constant vertical shear. The atmosphere is non-Boussinesq and continuous. The solution of this problem involves confluent hypergeometric functions, and the mathematical difficulty of the problem, for the most part, has precluded extracting simple results of some generality. In this note, it is shown that there does exist a very simple, powerful approximate result for the growth rate of the most rapidly growing instability, *viz.*, that this growth rate is linearly proportional to the surface meridional temperature gradient. The coefficient of proportionality is also easily determined. Moreover, the result extends to substantially more general profiles than those in the Charney problem.

1. Introduction

In this note we consider the instability of a purely baroclinic zonal flow (i.e., $\bar{u}$ depends only on height z). The equations and scalings used are well known. For the convenience of the reader these are reproduced in Section 2. It turns out that there exists a scaling for an unbounded, constant-shear, Boussinesq fluid which permits one to solve for stability properties at a single shear, on a β plane centered at a particular latitude in a fluid with a particular static stability—and to extend these results to any shear, latitude and static stability by means of the scaling relations. While this scaling is inapplicable for more general situations, we show that if one restricts oneself to the most rapidly growing disturbances, the scaling remains approximately correct under rather general conditions. This is shown in Section 3. In Section 4 the results from Section 3 are compared with numerical results. The latter support the scaling approximation. However, the numerical results suggest that the "exact" solutions are, in fact, simpler than those based on scaling.

0022-4928/80/071648-07$05.75

2. Equations and scalings

We restrict ourselves to pure baroclinic flows [i.e., $\bar{u} = \bar{u}(z)$] on a β plane and to quasi-geostrophic perturbations. The equations are derived and discussed in Charney (1947, 1973). Solutions have been presented not only in Charney (1947, 1973), but also by many others including Kuo (1952), Burger (1962), Miles (1964), Geisler and Garcia (1977), Green (1960) and Lindzen *et al.* (1980). As in most of these works, we will confine ourselves to configurations with a constant Brunt-Väisälä frequency N and a constant density scale height H. All our equations are in the form used in Lindzen *et al.* (1980). Although, Lindzen *et al.* were concerned with the role of wave-overreflection in baroclinic instability, that concept is not basic to the present work.

The equation for the geostrophic streamfunction ψ is

$$\psi_{zz} + \left(\frac{q_y(z)}{\bar{u} - c} - \frac{k^2}{\epsilon} - \frac{1}{4H^2}\right)\psi = 0, \tag{1}$$

where solutions of the form

$$\Psi = \psi(z)e^{z/2H}e^{ik(x-ct)} \tag{2}$$

have been assumed and where

$$q_y(z) = \frac{\beta}{\epsilon} + \frac{1}{H}\frac{d\bar{u}}{dz} - \frac{d^2\bar{u}}{dz^2}$$

$$= y - \left(\begin{array}{c}\text{derivative of}\\ \text{pseudo-potential}\\ \text{vorticity}\end{array}\right).$$

The terms have the following meanings:

H scale height for basic density (assumed constant) $[=RT_0/g]$
z height
ϵ f^2/N^2
f Coriolis parameter
β $\dfrac{df}{dy}$
x eastward distance.

Requiring the vertical velocity to vanish at the ground implies

$$\psi_z + \frac{1}{2H}\psi - \frac{\dfrac{d\bar{u}}{dz}}{\bar{u} - c}\psi = 0 \quad \text{at} \quad z = 0. \tag{3}$$

Various choices are possible for an upper boundary condition. For our numerical results we will assume a rigid lid at some $z = z_T$, i.e.,

$$\psi_z + \frac{1}{2H}\psi - \frac{\dfrac{d\bar{u}}{dz}}{\bar{u} - c}\psi = 0 \quad \text{at} \quad z = z_T. \tag{4}$$

As will be seen in Section 3, the presence or absence of such a lid is of little consequence to the specific results we seek. The equations for a Boussinesq fluid are obtained by letting $H \to \infty$ in Eqs. (1), (3) and (4).

Following Lindzen *et al.* (1980), we will first nondimensionalize the above equations. Let

$$m = \frac{d\bar{u}}{dz} \quad \text{at} \quad z = 0, \tag{5a}$$

$$u_0 = \bar{u} \quad \text{at} \quad z = 0. \tag{5b}$$

We then nondimensionalize as follows:

$$\tilde{u} \equiv \frac{\bar{u} - u_0}{mH}, \tag{6a}$$

$$\tilde{c} \equiv \frac{c - u_0}{mH}, \tag{6b}$$

$$\tilde{z} \equiv \frac{z}{H}, \tag{6c}$$

$$\alpha^2 \equiv \frac{k^2H^2}{\epsilon}. \tag{6d}$$

From (6a), (5a) and (5b) we also have

$$\frac{d\tilde{u}}{d\tilde{z}} = 1 \quad \text{at} \quad \tilde{z} = 0, \tag{7a}$$

$$\tilde{u} = 0 \quad \text{at} \quad \tilde{z} = 0. \tag{7b}$$

Eqs. (1), (3) and (4) become

$$\psi_{\tilde{z}\tilde{z}} + \left(\frac{r + \dfrac{d\tilde{u}}{d\tilde{z}} - \dfrac{d^2\tilde{u}}{d\tilde{z}^2}}{\tilde{u} - \tilde{c}} - \alpha^2 - \frac{1}{4}\right)\psi = 0, \tag{8}$$

$$\psi_{\tilde{z}} + \tfrac{1}{2}\psi + \frac{1}{\tilde{c}}\psi = 0 \quad \text{at} \quad \tilde{z} = 0, \tag{9}$$

$$\psi_{\tilde{z}} + \tfrac{1}{2}\psi - \frac{\dfrac{d\tilde{u}}{d\tilde{z}}}{\tilde{u} - \tilde{c}}\psi = 0 \quad \text{at} \quad \tilde{z} = \frac{z_T}{H}, \tag{10}$$

where

$$r \equiv \frac{\beta H}{\epsilon m}. \tag{11}$$

We will now, temporarily, restrict ourselves to the Charney problem where $d\tilde{u}/d\tilde{z} = 1$. Eqs. (8), (9) and (10) become

$$\psi_{\tilde{z}\tilde{z}} + \left(\frac{r + \boxed{1}}{\tilde{z} - \tilde{c}} - \alpha^2 - \boxed{\frac{1}{4}}\right)\psi = 0, \tag{12}$$

$$\psi_{\tilde{z}} + \boxed{\frac{1}{2}\psi} + \frac{1}{\tilde{c}}\psi = 0 \quad \text{at} \quad \tilde{z} = 0, \tag{13}$$

$$\psi_{\tilde{z}} + \boxed{\frac{1}{2}\psi} - \frac{1}{\tilde{z} - \tilde{c}}\psi = 0$$

at

$$\tilde{z} = \tilde{z}_T = \frac{z_T}{H}. \tag{14}$$

Boxed terms disappear in a Boussinesq fluid. Note also that all information concerning shear, latitude and static stability is incorporated into the single parameter r (and, of course, in the nondimensionalization).

We next rescale Eqs. (12)–(14) as follows:

$$\hat{z} = (r + 1)\tilde{z}, \tag{15a}$$

$$\hat{c} = (r + 1)\tilde{c}, \tag{15b}$$

and

$$\delta^2 = \frac{\alpha^2 + \boxed{\frac{1}{4}}}{(r + \boxed{1})^2}. \tag{15c}$$

Eqs. (12)–(14) become

$$\psi_{\hat{z}\hat{z}} + \left(\frac{1}{\hat{z} - \hat{c}} - \delta^2\right)\psi = 0, \tag{16}$$

$$\psi_{\hat{z}} + \left(\frac{1}{\hat{c}} + \boxed{\frac{1}{2(r + 1)}}\right)\psi = 0 \quad \text{at} \quad \hat{z} = 0, \tag{17}$$

$$\psi_{\hat{z}} + \left(-\frac{1}{\hat{z} - \hat{c}} + \boxed{\frac{1}{2(r + 1)}}\right)\psi = 0$$

at

$$\hat{z} = \hat{z}_T = (r + 1)\hat{z}_T. \tag{18}$$

Once again, boxed terms are omitted in a Boussinesq fluid. Note that for a Boussinesq fluid, r is absent from Eqs. (16)–(18)—entering only into the determination of $\hat{z}_T$. Thus, for an *unbounded* Boussinesq fluid one could solve Eqs. (16)–(17) once, and use the scaling relations (15a)–(15c) to obtain the solution *exactly* for any choice of r. This can no longer be done exactly in the above system because of 1) non-Boussinesq terms in the boundary conditions; and 2) the presence of a lid at a finite height.

The latter difficulty may seem artificial since the atmosphere does not have a lid. However, an identical scaling breakdown occurs if the constant shear ceases (or even changes) above some height. The purpose of the next two sections is to show that the scaling results still hold approximately under a variety of conditions.

3. Approximate scaling for maximum growth rate

For the moment, let us assume we do have an unbounded Boussinesq fluid [assume solutions are bounded as $\hat{z} = \infty$ in lieu of Eq. (18)]. Then, from Eqs. (16) and (17) we can obtain $\delta\hat{c}_i$ (where $\hat{c}_i$ is the imaginary part of $\hat{c}$; positive $\hat{c}_i$ corresponds to instability) as a function of δ. There will exist a unique δ for which $\delta\hat{c}_i$ has its largest value $(\delta\hat{c}_i)_{\max}$. We call this δ, $\delta_{\max}$. From the scaling relations (15a) and (15c) we have

$$\tilde{c} = \frac{\hat{c}}{r}, \tag{19a}$$

$$\alpha = r\delta. \tag{19b}$$

Hence, the maximum nondimensional growth rate will simply be

$$(\alpha\tilde{c}_i)_{\max} = (\delta\hat{c}_i)_{\max} \tag{20a}$$

independent of r and will occur at

$$\alpha_{\max} = r\delta_{\max}. \tag{20b}$$

The dimensional form of (20) obtained from (6b) and (6d) is then

$$(kc_i)_{\max} = \epsilon^{1/2} m(\delta\hat{c}_i)_{\max}. \tag{21}$$

$(\delta\hat{c}_i)_{\max}$ is a single number that can be obtained once and for all (it turns out to be ~ 0.31). Eq. (21) is then an extraordinarily simple expression for the maximum growth rate for any shear, latitude and static stability.

In Section 3 we noted two reasons why this scaling breaks down for the non-Boussinesq problem considered there. An additional difficulty arises from the fact that in a non-Boussinesq fluid (15c) no longer implies that δ and α are linearly proportional. Instead,

$$\alpha = \delta(r + 1)\left[1 - \frac{1}{4\delta^2(r + 1)^2}\right]^{1/2}. \tag{22}$$

Clearly, for small $\delta^2(r + 1)^2$, the last factor on the right-hand side of (22) will differ substantially from unity. Indeed, we see that *no* real α's will correspond to δ's such that

$$\delta < \frac{1}{2(r + 1)}. \tag{23}$$

A consequence of this is that $(\alpha\tilde{c}_i)_{\max}$ will no longer occur at that α corresponding to $\delta_{\max}$. The above simply renders the scaling results more complicated.

In the remainder of this section we will examine each of the three difficulties to see whether they are fatal to a result like Eq. (21). First, it should be noted that there is no difficulty in solving (1), subject to any reasonable boundary conditions, numerically. Effective methods are described in Lindzen *et al.* (1980) and Geisler and Garcia (1977). The method in Lindzen *et al.* (1980) has, in fact, been used to solve for $\hat{c}(\delta)$ for the unbounded Boussinesq problem. Results are shown in Fig. 1 for $\hat{c}_r(\delta)$, $\hat{c}_i(\delta)$ and $\delta\hat{c}_i(\delta)$ in the neighborhood of $\delta_{\max}$. (Note that $\delta_{\max} \approx 0.777 > 0.5$. From (23) we see that there will always be an α corresponding to $\delta_{\max}$.) These results will be needed later in this section. The virtue of

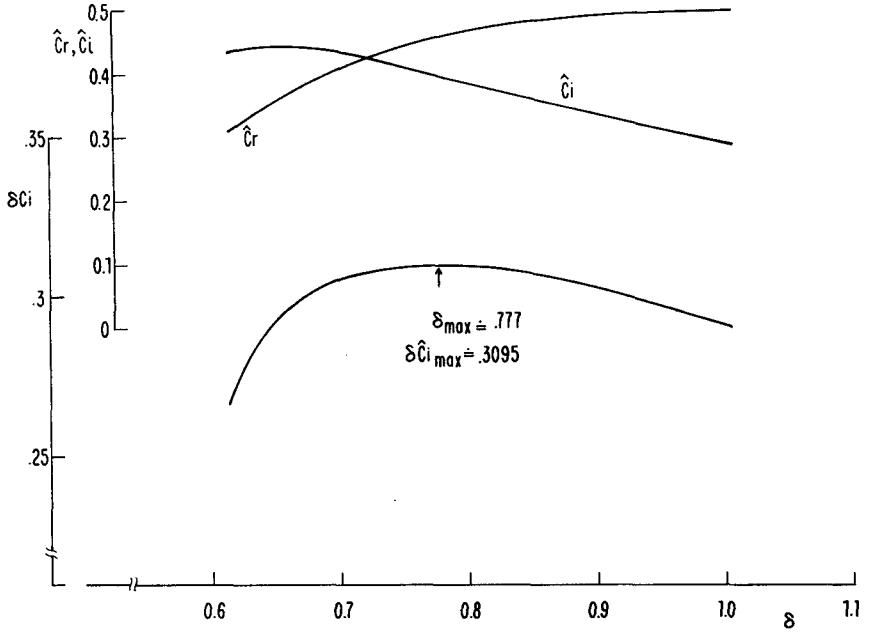

FIG. 1. $\hat{c}_r$, $\hat{c}_i$ (real and imaginary parts of $\hat{c}$) and $\delta\hat{c}_i$ vs δ (see text for definitions).

Eq. (21) arises *not* because of any inability to solve Eq. (1), but because its simplicity allows us to determine important information about stability immediately, virtually without calculation. Another preliminary remark emerges from inspection of Eqs. (16)–(18), namely, the non-Boussinesq problem asymptotically approaches the unbounded Boussinesq case for *large* r (i.e., small shear). Thus, our concern will be with *small* values of r.

We will first consider the presence of the non-Boussinesq term in the lower boundary condition, Eq. (17). From Fig. 1 we see that in the neighborhood of $\delta_{\max}$ (in fact, for $\delta \geq 0.5$), $\hat{c}_r \leq 0.5$, $\hat{c}_i \leq 0.45$, and $|\hat{c}^{-1}| \geq 1.5$, while $1/[2(r+1)] < 0.5$. Clearly, the non-Boussinesq term is always *less* than one-third the magnitude of the remaining term, and for large r the inequality is even stronger. Since the non-Boussinesq term constitutes a non-singular perturbation we reasonably expect its neglect to lead to errors on the order of 30% or less.

We turn next to the upper boundary condition. From Eq. (16) we see that the factor in parentheses has a turning point when

$$\hat{z} = \hat{z}_t = \hat{c} + \frac{1}{\delta^2}. \tag{24}$$

From Fig. 1 we see that $\delta_{\max} \approx 0.777$ and $\delta_{\max}^{-2} \approx 1.656$. For $\delta \approx \delta_{\max}$,

$$\hat{z}_t = \hat{c}_r + i\hat{c}_i + \frac{1}{\delta^2}$$
$$= 2.12 + i(0.395). \tag{25}$$

Although, $\hat{c}$ is complex, $\hat{z}_t$ is very nearly real. As noted in Lindzen *et al.* (1980), $\hat{z}_t$ represents an effective top to a region of vertical wave propagation existing between the critical layer ($\hat{z} \approx \hat{c}_r$) and z_t. Above z_t, these internal waves are trapped, and hence, the role of boundaries (or other features) above z_t on the solution below z_t is small. It is the solution below z_t which is germane to stability properties. The arguments in Lindzen *et al.* (1980) were developed for $c_i = 0$. While $c_i \neq 0$, here, it is clear from (25) that c_i is merely a perturbation to the real part of the Doppler-shifted phase speed at z_t, and hence, the above physics remains relevant. Thus we expect, *a priori*, that the effects of upper boundaries, upper boundary conditions, and even the deviation of $\bar{u}$ from constant shear will be of little importance provided they occur above $\hat{z} = \hat{z}_t$. From Eq. (15a) we have that $\tilde{z} = \hat{z}/(r+1)$. Thus, anything above $\tilde{z} \approx 2.12$ should be of little consequence regardless of r. In the next section we will consider a mean zonal flow where the mean shear goes to zero above $\tilde{z} = 1$. *A priori* we expect this, too, to be of little consequence for $r \geq 1$. In fact, numerical results show it to be unimportant for all r's. We suspect that this is due to the fact that for the most rapidly growing mode, the presence of c_i leads to marked decay with height even below z_t.

The above discussion implies that, given the results in Fig. 1 for $(\delta\hat{c}_i)_{\max}$, we may extend them (at least approximately) by means of the scaling relations (15b) and (22), to the Charney problem at any value of r (even with an upper lid). There only

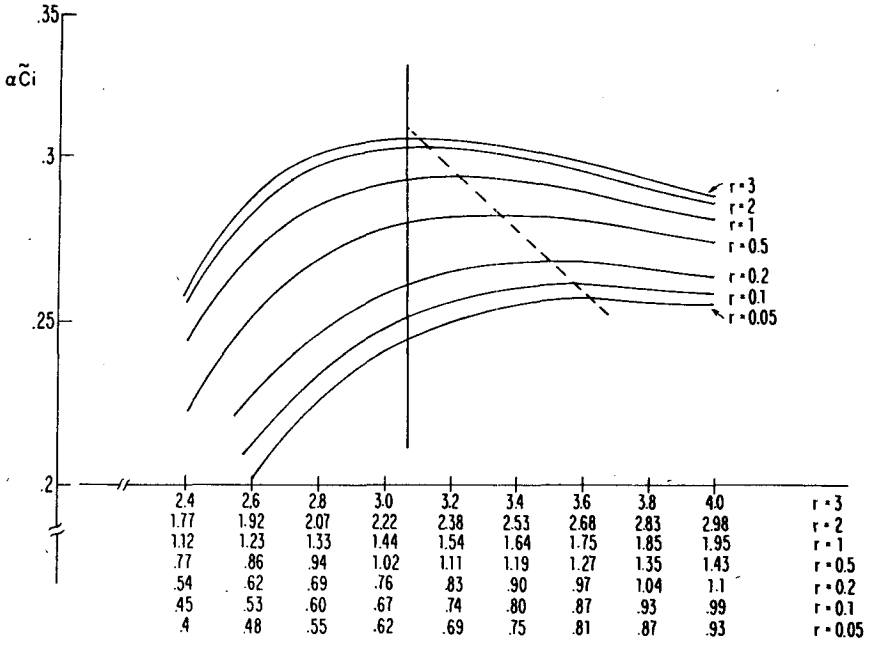

FIG. 2. $\alpha\tilde{c}_i$ vs α for various choices of r as obtained by scaling the results in Fig. 1. The vertical line corresponds to δ_{max}. The dashed line is the locus of α_{max}. Note that the α-scales are slightly nonlinear in α; they are linear in δ.

remains the technical point, mentioned earlier in this section, that α is not linearly proportional to δ, and, therefore, the maximum in $\alpha\tilde{c}_i$ will not correspond exactly to the maximum of $\delta\hat{c}_i$. This is seen most clearly by combining Eqs. (15b) and (22):

$$\alpha\tilde{c}_i = \delta\hat{c}_i\left[1 - \frac{1}{4\delta^2(r+1)^2}\right]^{1/2}. \qquad (26)$$

If the factor in square brackets were unity then (26) would reduce to (20a) and $(\alpha\tilde{c}_i)_{max}$ would equal $(\delta\hat{c}_i)_{max}$ and would occur at that value of α corresponding to δ_{max}. From (26) we see that for finite r, $(\alpha\tilde{c}_i)_{max}$ will be smaller than $(\delta\hat{c}_i)_{max}$, and will occur for values of α corresponding to δ's greater than δ_{max}. This is quantitatively displayed in Fig. 2, where we use the results from Fig. 1, scaled according to Eqs. (22) and (26) to plot $(\alpha\tilde{c}_i)$ vs α at various r's. The reader should note that Fig. 2 shows only a very restricted range of $(\alpha\tilde{c}_i)$'s. The results in this figure are consistent with the claim that $(\alpha\tilde{c}_i)_{max}$ is a constant independent of r to within ±9%.

4. Numerical comparisons and conclusions

In order to check the approximate scaling results described in Sections 2 and 3, we solved Eqs. (8), (9) and (10) numerically for various values of r ranging from $r = 0.05$ to $r = 3$, with a rigid lid at $\tilde{z} = \tilde{z}_T = 4$. In addition to the Charney profile where $\tilde{u}_{\tilde{z}} = 1$, we also considered a set of profiles wherein

$$\tilde{u}_{\tilde{z}} = \frac{1}{2}\left[1 - \tanh\left(\frac{\tilde{z} - \tilde{z}_B}{\tilde{l}}\right)\right].$$

In such profiles $\tilde{u}_{\tilde{z}}$ undergoes a smooth transition in a region $\pm\tilde{l}$ about $\tilde{z} = \tilde{z}_B$ from approximately 1 below this region to approximately zero above this

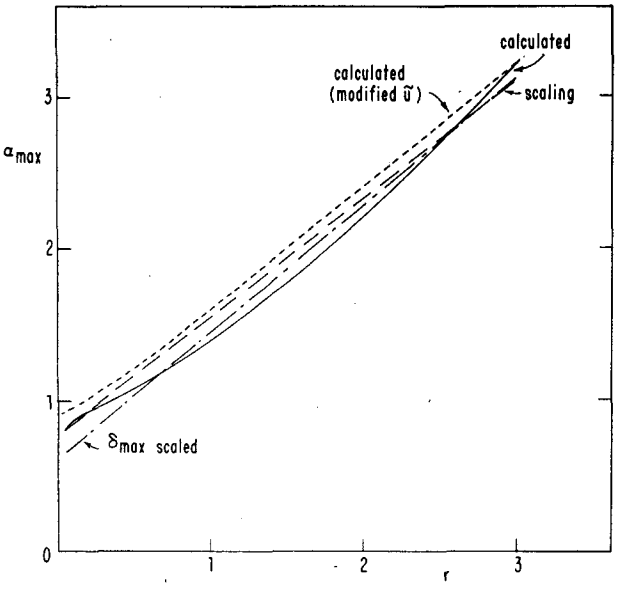

FIG. 3. α_{max} vs r from numerical calculations for a profile with constant shear and for a profile with constant shear up to $\tilde{z} = 1.5$ and no shear above. Also shown are scaling results based on Fig. 2 as well as the scaling of δ_{max}.

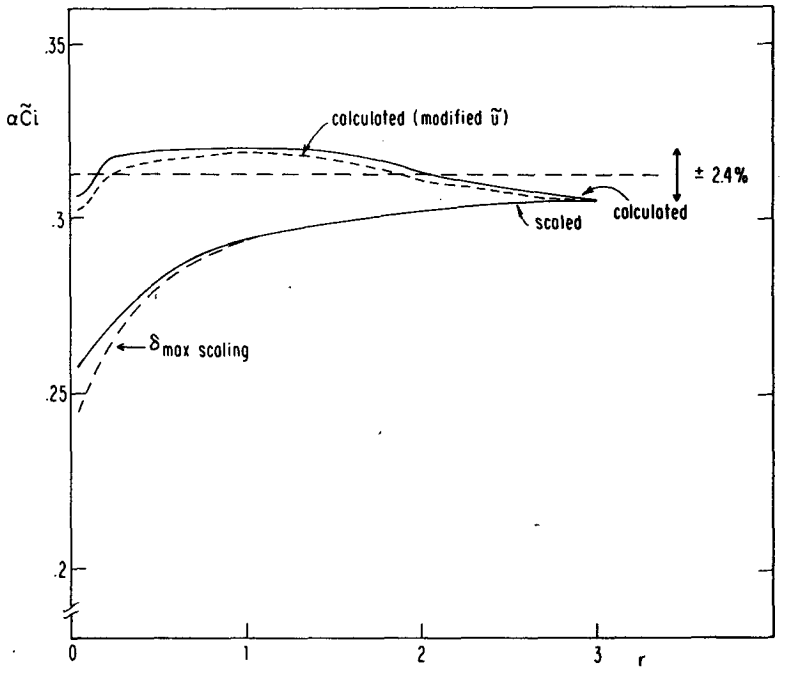

FIG. 4. $(\alpha\tilde{c}_i)_{\max}$ vs r for the four cases described in Fig. 3.

region. Clearly, $\tilde{u}_{\tilde{z}\tilde{z}}$ is no longer zero, and the full version of Eq. (8) was used. Numerical calculations were performed for values of $\tilde{l}$ varying from 0.25 to 0.00625[1] and values of $\tilde{z}_B$ from 1 to 2. As concerns the most rapidly growing mode, such variations yielded negligible differences, and, consequently, we display results from the case $\tilde{z}_B = 1.5$ and $\tilde{l} = 0.0125$.

In Fig. 3 we show the value of α for which $(\alpha\tilde{c}_i)$ is a maximum $\alpha_{\max}$ as a function of r. Four curves are shown: two correspond to the numerical results for the Charney profile of $\tilde{u}(\tilde{z})$ and the modified profile described above. The third curve shows the value of $\alpha_{\max}$ determined from the scaling results shown in Fig. 2. The fourth curve is obtained by scaling $\delta_{\max}$ according to Eq. (22). All four curves are exceedingly similar. There is rather little difference in the numerical results for the two $\tilde{u}(\tilde{z})$ profiles; in terms of percentage accuracy, the scaled results from Fig. 2 are closer to the numerical results than are the results based on the simple scaling of $\delta_{\max}$. The difference, however, is not great.

In Fig. 4 we show $(\alpha\tilde{c}_i)_{\max}$ vs r for the four cases described above. Numerical results for the two profiles of $\tilde{u}(\tilde{z})$ are almost identical. So too are the scaling results and the results based on simply scaling $(\delta\hat{c}_i)_{\max}$. The two pairs of results differ by about the error estimate obtained by comparing $|1/\hat{c}|$ and $1/2(r + 1)$ in Eq. (17). The most interesting result in Fig. 4 is that $(\alpha\tilde{c}_i)_{\max}$ obtained from explicit numerical calculations is much more nearly independent of r than are the scaling results. From the numerical results we find

$$(\alpha\tilde{c}_i)_{\max} \approx 0.3125 \pm 0.0075 \qquad (27)$$

regardless of r. The numerical results are obviously more accurate than the scaling arguments of Section 3. The latter serves only as a partial explanation of the somewhat surprising numerical result given by (27).

Using (6b) and (6d) to express (27) in dimensional terms, we get

$$(kc_i)_{\max} = \sqrt{\epsilon}\, m = 0.3125 = \frac{f}{N}\frac{d\bar{u}}{dz}\bigg|_{z=0} \times 0.3125. \qquad (28)$$

Of course, our numerical results are based on profiles where $d\bar{u}/dz$ was almost constant throughout the bulk of the troposphere. However, the results of Geisler and Garcia (1977) suggest that (28) *may* be substantially more general. Geisler and Garcia (1977) calculated the baroclinic instability of a variety of profiles $\bar{u}(z)$ which differed widely except for the value of $d\bar{u}/dz$ at the ground. The distribution of kc_i as a function of k was also different for each profile. However, to the accuracy with which one may read the diagrams in Geisler and Garcia (1977), the value of $(kc_i)_{\max}$ was identical for each profile and was given by (28). In some of our own calculations (which we expect to present separately) an

[1] For these profiles $\tilde{u}_{\tilde{z}}$ is not exactly unity at $\tilde{z} = 0$. Appropriate corrections to r were made.

exception to the generality of (38) did emerge. In all the profiles considered here, q_y [see Eq. (1)] is everywhere positive. As noted in Lindzen and Tung (1978), the existence of instabilities arises from the existence of what is effectively a negative delta function in q_y at the ground. If one considers profiles where $u_z = 0$ at $z = 0$ and where there is a layer of negative q_y merging into a more normal region of positive q_y at some height z_M, then (28) holds provided one uses du/dz at $z = z_M$, and provided that the negative q_y is not very close to zero. As q_y becomes nearly zero in the region of negative q_y, the growth rate precipitously goes to zero. Such profiles are sufficiently anomalous to render detailed discussion of them here unwarranted. Almost all profiles considered in the present literature have positive q_y throughout the troposphere, and finite positive shear at the ground.

An especially simple form of (28) may be obtained by using an approximate form of the thermal wind relation:

$$\frac{d\bar{u}}{dz} \cong -\frac{g}{f\bar{T}}\frac{\partial \bar{T}}{\partial y}, \tag{29}$$

where y = northward distance. Substituting (29) into (28) we get

$$(kc_i)_{\max} = -\left(0.3125 \times \frac{g}{\bar{T}N}\right)\frac{\partial \bar{T}}{\partial y}\bigg|_{z=0} \tag{30a}$$

$$= -\left(0.3125 \times \frac{g}{a\bar{T}N}\right)\frac{\partial \bar{T}}{\partial \phi}\bigg|_{z=0} \tag{30b}$$

where a is the earth's radius and ϕ the latitude in radians.

Note that the quantity in parentheses in both (30a) and (30b) is very nearly a constant independent of f and hence, latitude. This factor is easily evaluated. Taking

$$g = 9.8 \text{ m s}^{-2},$$

$$\bar{T} \approx 290 \text{ K},$$

$$\frac{d\bar{T}}{dz} + \frac{g}{cp} \approx 3.3 \text{ K km}^{-1},$$

$$a \approx 6.4 \times 10^3 \text{ km},$$

we get

$$(kc_i)_{\max} \approx \frac{-\left.\dfrac{\partial \bar{T}}{\partial \phi}\right|_{z=0}}{74.1 \text{ K day}}. \tag{30c}$$

That (30c) is independent of latitude is, of course, somewhat misleading. Eq. (30c) assumes that the values of k for which $(kc_i)_{\max}$ is achieved is physically realizable. For example, as we approach the poles the length of a latitude circle and the distance to the pole become too small to contain $k_{\max}$. These kinematic effects do not appear important below 64° latitude. What happens above this latitude band, while of considerable importance, is beyond the scope of this note.

Acknowledgments. This work has been supported by the National Science Foundation under Grant ATM-78-23330 and by the National Aeronautics and Space Administration under Grant NGL-22-007-228. The authors also wish to thank Dr. I. M. Held for pointing out to them the scaling properties of the unbounded Boussinesq case.

REFERENCES

Burger, A. P., 1962: On the non-existence of critical wavelengths in a continuous baroclinic stability problem. *J. Atmos. Sci.*, **19**, 31–38.

Charney, J. G., 1947: The dynamics of long waves in a baroclinic westerly current. *J. Meteor.*, **4**, 135–162.

——, 1973: Planetary fluid dynamics. *Dynamic Meteorology*, P. Morel, Ed. D. Reidel, 97–351.

Geisler, J. E., and R. Garcia, 1977: Baroclinic instability at long wavelengths on a β plane. *J. Atmos. Sci.*, **34**, 311–321.

Green, J. S. A., 1960: A problem in baroclinic stability. *Quart. J. Roy. Meteor. Soc.*, **86**, 237–251.

Kuo, H. L., 1952: Three-dimensional disturbances in a baroclinic zonal current. *J. Meteor.*, **9**, 260–278.

Lindzen, R. S., and K.-K. Tung, 1978: Wave over-reflection and shear instability. *J. Atmos. Sci.*, **35**, 1626–1632.

——, B. Farrell and K.-K. Tung, 1980: The concept of wave-over-reflection and its application to baroclinic instability. *J. Atmos. Sci.*, **37**, 44–63.

Miles, J. W., 1964: Baroclinic instability of the zonal wind. *Rev. Geophys.*, **2**, 155–176.